Preclinical evaluation of new α-radionuclide therapy targeting LAT1: 2-[211At]astato-α-methyl-L-phenylalanine in tumor-bearing model

Yasuhiro OHSHIMA (ohshima.yasuhiro@qst.go.jp)
National Institutes for Quantum and Radiological Science and Technology https://orcid.org/0000-0001-6605-3779

Hiroyuki Suzuki
Graduate School of Pharmaceutical Science, Chiba University

Hirofumi Hanaoka
Gunma University Graduate School of Medicine

Ichiro Sasaki
National Institutes for Quantum and Radiological Science and Technology

Shigeki Watanabe
National Institutes for Quantum and Radiological Science and Technology

Hiromitsu Haba
Nishina Center for Accelerator-Based Science, RIKEN

Yasushi Arano
Graduate School of Pharmaceutical Science, Chiba University

Yoshito Tsushima
Gunma University Graduate School of Medicine

Noriko S. Ishioka
National Institutes for Quantum and Radiological Science and Technology

Original research

Keywords: α-emitter, targeted radionuclide therapy, L-type amino acids transporter 1 (LAT1), 2-[211At]astato-α-methyl-L-phenylalanine ([211At]-2-AAMP)

Posted Date: March 13th, 2020

DOI: https://doi.org/10.21203/rs.3.rs-17079/v1

Version of Record: A version of this preprint was published at Nuclear Medicine and Biology on November 1st, 2020. See the published version at https://doi.org/10.1016/j.nucmedbio.2020.08.003.

Abstract

PURPOSE: Targeted α-radionuclide therapy has growing attention as a promising therapy for refractory cancers. However, the application is limited to certain types of cancer. Since L-type amino acids transporter 1 (LAT1) is highly expressed in various human cancers, we prepared LAT1-selective α-emitting amino acid analog, 2-[211At]astato-α-methyl-L-phenylalanine ([211At]-2-AAMP), and evaluated its potential as a therapeutic agent.

METHODS: [211At]-2-AAMP was prepared from the stannyl precursor. Stability of [211At]-2-AAMP was evaluated by both in vitro and in vivo. In vitro studies using LAT1 expressing human ovary cancer cell line, SKOV3, were performed for evaluating cellular uptake and cytotoxicity of [211At]-2-AAMP. Biodistribution and therapeutic studies in SKOV3 bearing mice were performed after intravenous injection of [211At]-2-AAMP.

RESULTS: [211At]-2-AAMP was stable in murine plasma in vitro and excreted into urine as intact. Cellular uptake of [211At]-2-AAMP was inhibited by treatment with LAT1-selective inhibitor. After 24 hours of incubation, [211At]-2-AAMP suppressed clonogenic growth at 10 kBq/ml, and induced cell death and DNA double strand break at 25 kBq/ml. When injected to mice, [211At]-2-AAMP exhibited the peak accumulation in the tumor at 30 min postinjection, and the radioactivity levels in the tumor retained up to 60 min. The majority of the radioactivity was rapidly eliminated from the body into the urine as an intact form immediately after injection. [211At]-2-AAMP significantly improved the survival of mice ($P<0.05$) without serious side effects.

CONCLUSION: [211At]-2-AAMP showed α-radiation-dependent cellular growth inhibition after taking up via LAT1. Furthermore, [211At]-2-AAMP provided a beneficial effect on survival in vivo. These findings suggest that [211At]-2-AAMP might be useful for treatment of LAT1-positive cancer.

Introduction

Targeted radionuclides therapy with α-emitters has drawn global attention. Linear energy transfer (LET) of α-particle is approximately 80 keV/μm, and thus α-radiation is considered to be high-LET radiation [1, 2]. According to the lots of studies with external beam irradiation, high-LET radiation can induce irreparable DNA double-strand breaks and effectively lead cell death compared to low-LET radiation [1, 3]. In addition, path-length of α-particle in water is short (50 ~ 100 μm) [1, 2]. These characteristics are beneficial in eliminating tumors and reducing damages in normal tissues surrounding the tumor. Allen BJ et al. has reported that the therapeutic effects with α-emitter were superior to those of β-emitter in vitro, in vivo, and in clinical [4]. More than ten clinical studies have shown the significant improvements of survival after treatment with α-emitter labeled carriers targeting specific molecules for cancer, such as CD33, prostate specific membrane antigen (PSMA), and somatostatin receptor (SSTR) [5–7]. However, the application of these radiopharmaceuticals is limited to certain types of cancers expressing these

target molecules. Radiopharmaceuticals targeting molecules that express on various types of cancers would enable the wider use of targeted α-therapy.

To support the abnormal growth of tumor, several types of amino acid transporters are highly expressed than normal cells. Among them, L-type amino acids transporter 1 (LAT1) has significant roles for cancer growth and survival through efficient supply of amino acids and activation of mammalian target of rapamycin (mTOR) signaling known as a master regulator of cell growth [8]. LAT1 couples with CD98 on the plasma membrane for its functional expression and transports neutral essential amino acids sodium-independently [9]. LAT1 is highly expressed in various types of human cancer, therefore, α-radionuclide therapy targeting LAT1 might be useful for broad range of cancers [10].

We previously developed fluorine-18 (^{18}F)- or bromine-76 (^{76}Br)-labeled amino acid tracers targeting LAT1 [11–14]. Among them, 2-[^{18}F]fluoro-α-methyl-L-phenylalanine ([^{18}F]-2-FAMP) and 2-[^{76}Br]bromo-α-methyl-L-phenylalanine ([^{76}Br]-2-BAMP) were specifically taken up by tumor via LAT1 and retained in tumor, while they were rapidly cleared from body and excreted into urine. Since ^{18}F and ^{76}Br belong to radiohalogen, astatine-211 (^{211}At, half-life: 7.2 h), an attractive α-emitter of halogen, labeled α-methyl-L-phenylalanine is expected to show high tumor accumulation and preferred pharmacokinetics. In this study, we newly synthesized 2-[^{211}At]astato-α-methyl-L-phenylalanine ([^{211}At]-2-AAMP), and characterized its stability, LAT1-specific cellular uptake and biodistribution in tumor-bearing mice. Furthermore, therapeutic effects of [^{211}At]-2-AAMP were evaluated both in vitro and in vivo.

Materials And Methods

General

A reversed-phase HPLC (RP-HPLC) analysis was performed with a C18 column (Capcell Pak C18 AQ, 4.6 × 250 mm; Shiseido Co., Tokyo, Japan) at a flow rate of 1 ml/min eluted with a linear gradient of 0.1% aqueous trifluoroacetic acid (TFA) and acetonitrile with 0.1%TFA from 90:10 to 0:100 for 30 min. Thin-layer chromatography (TLC) was developed with a mixture of 1-butanol, acetic acid and water (4:1:1, v/v/v). The TLC was visualized and quantified using an imaging scanner (Typhoon FLA7000, GE Healthcare Japan, Tokyo, Japan). The stannyl precursor of [^{211}At]-2-AAMP was synthesized according to the procedure described previously [13]. 2-Iodo-a-methyl-L-phenylalanine (2-IAMP) was supplied from Nagase Sangyo (Tokyo, Japan)

Radiolabeling

^{211}At was produced via the ^{209}Bi(a,2n)^{211}At reaction and isolated by the dry distillation [15]. The detailed procedures were described in Detailed Materials and Methods (see Online Resource). For preparation of [^{211}At]-2-AAMP, the protected compound of [^{211}At]-2-AAMP (Prot-[^{211}At]-2-AAMP) was prepared and then used for the following deprotection reaction without purification. (Fig. 1). To a solution of the stannyl precursor in methanol containing 1% acetic acid (100 μg/450 μl) was added an aqueous solution of ^{211}At

(150 µl) and subsequently a solution of *N*-chlrosuccinimide (NCS) in methanol (100 µg/10 µl). After the mixture was allowed to stand for 15 min at room temperature, an aqueous solution of sodium bisulfite (200 µg/10 µl) and subsequently 6 N NaOH (620 µl) was added. After the reaction for 1 h at 70°C, 6 N HCl was added to the mixture at 0°C to adjust pH between 2 and 7. The mixture was analyzed by TLC before RP-HPLC purification to determine the radiochemical yield. The eluent of RP-HPLC was collected at 1 min intervals in each tube containing 10% aqueous solution of ascorbic acid (10 µl). The fractions containing the product was identified by comparing the retention time of 2-IAMP, and was concentrated in vacuo. Then, remained solution was applied to a Sep-pak C18 cartridge preconditioned with methanol and water. The cartridge was washed with water (2 ml), and eluted with methanol (1 ml). After the eluent was added 10% aqueous solution of ascorbic acid (10 µl), the solvent was removed in vacuo. Radiochemical purity was determined by TLC and RP-HPLC.

Stability assessments of [^{211}At]-2-AAMP

Animal experimental protocol was approved by the Institutional Animal Care and Use Committee at our facility (19-T001-1), and all animal experiments were conducted in accordance with the institutional guidelines regarding animal care and handling. For the evaluation of *in vitro* stability, each 50 µl aliquot of [^{211}At]-2-AAMP in phosphate buffered saline (PBS) (2.4 MBq/ml) was added to a freshly prepared murine plasma (450 µl). After the mixture was incubated for 6 h at 37°C, a 2 µl aliquot of each sample was analyzed by TLC. For the evaluation of *in vivo* stability, urine was collected up to 1 h after intravenous injection of [^{211}At]-2-AAMP (100 kBq) in 100 µl of PBS into six-week-old male ICR normal mice (CLEA Japan, Tokyo, Japan). A 2 µl aliquot of each urine sample was analyzed by TLC.

Cellular uptake and release of [^{211}At]-2-AAMP

SKOV3, a human ovarian adenocarcinoma cell line, was obtained from American Type Culture Collection (Manassas, VA, USA). The procedure for cell culture was shown in Detailed Materials and Methods (see Online Resource). Cells (1.0×10^5 cells/well) were seeded in the 24-well plates and incubated in the growth medium for 24 h. For a time-course study, cells were washed with Hanks' balanced salt solution (HBSS) two times, then incubated in HBSS containing [^{211}At]-2-AAMP at 37^{o}C for 10, 20, 30, 60 and 90 min. For examining sodium-independency, SKOV3 was incubated with [^{211}At]-2-AAMP in HBSS or sodium-free HBSS at 37^{o}C for 10 min. To investigate uptake pathway of [^{211}At]-2-AAMP, cells were incubated with [^{211}At]-2-AAMP containing various inhibitors for 10 min. [^{211}At]-2-AAMP uptake was terminated by removing the [^{211}At]-2-AAMP solution, followed by washing cells three times with ice-cold PBS. Cells were solubilized with 0.1 N NaOH and the radioactivity was measured with a well-type g-counter (ARC-7001, Hitachi-Aloka Medical, Tokyo, Japan). For examining extracellular release, SKOV3 cells were incubated in HBSS containing [^{211}At]-2-AAMP for 10 min. After 2 times washes with HBSS, cells were incubated in HBSS at 37^{o}C for 10, 20, 30, and 60 min. Then, supernatant was collected, and the radioactivity was measured with a well-type g-counter.

Immunoblotting

Cells were dissolved in sample buffer (25% glycerin, 1% SDS, 62.5 mM Tris-Cl, 10 mM dithiothreitol) and incubated at 65^{o}C (LAT1) or 95^{o}C (CD98) for 15 min. Aliquots of samples containing 20 μg of protein were analyzed by 10% SDS-polyacrylamide gel electrophoresis and transferred onto a polyvinylidene difluoride membrane. Blots were incubated at 4^{o}C overnight in 10 mM Tris–HCl, 100 mM NaCl, 0.1% Tween 20, pH 7.5 (TBST), with 5% skim milk. Then, blots were incubated with rabbit anti-LAT1 carboxyl-terminal antibody (1:5000 dilution), rabbit anti-LAT1 amino-terminal antibody (1:5000 dilution), or rabbit anti-CD98 antibody (1:200 dilution, Santa Cruz Biotechnology Inc, Santa Cruz, CA, USA) at 4^{o}C overnight [9, 16]. After washing with TBST, the blots were incubated with horseradish peroxidase conjugated anti-rabbit IgG antibody (1:20000 dilution, Cell Signaling Technology, Beverly, MA, USA) for 1.5 h at room temperature. The blots were further washed with TBST, and specific proteins were visualized by using enhanced chemiluminescence western blotting detection reagents (GE Healthcare).

Colony assay

Cells (1×10^{6} cells/dish) were pre-incubated in the growth medium for 24 h, and treated with 0, 10, 25, and 50 kBq/ml of [^{211}At]-2-AAMP for 24 h. After [^{211}At]-2-AAMP treatment, cells were washed with PBS, suspended in growth medium, and seeded at 200 cells/well in 6-well plate. Then, cells were incubated at 37^{o}C for 14 days. After incubation, cells were washed with PBS twice and stained with crystalviolet solution (6% glutaraldehyde, 0.5% crystalviolet). After washing cells with tap-water, the number of colonies (> 50 cells) were counted.

Lactate dehydrogenase (LDH) release assay

Cells (1×10^{4} cells/well) were pre-incubated for 24 h in a 96-well culture plate and treated with 0, 10, 25 and 50 kBq/ml of [^{211}At]-2-AAMP for 24 h. At the end of incubation, supernatants were collected and the LDH content was measured by using a Cytotoxicity Detection Kit (Roche Applied Sciences, Laval, Quebec, Canada). LDH release is expressed as percent of total content, which was determined by lysing an equal amount of cells with 1% Triton X-100.

DNA double-strand break (DSB) assay

Cells (1x10^{6} cells/dish) treated with [^{211}At]-2-AAMP (25 kBq/ml) for 24 h. Then neutral comet assay was applied to detect DNA-DSB using a CometAssay Kit (Trevigen, Gaithersburg, MD, USA) according to the manufacturer's instructions. Comet tails were stained with SYBR Green and analyzed using a fluorescent microscope.

Biodistribution study

Cells (5×10^{6} cells/head) were implanted into the right thigh of the five-week-old female BALB/c nude mice (CLEA Japan). When palpable tumors developed, [^{211}At]-2-AAMP (100 kBq) in 100 μl of PBS was intravenously injected. At selected time points after administration, the mice were euthanized, and the

tissues of interest were dissected and weighed. The radioactivity was measured by a well-type g-counter. The uptake of [^{211}At]-2-AAMP was expressed as a percentage of the injected dose per gram of organ.

Therapeutic study *in vivo*

Tumor-bearing mice were prepared in the same manner to biodistribution study. After tumor volumes had reached approximately 200 mm^3, [^{211}At]-2-AAMP therapy was conducted. PBS or [^{211}At]-2-AAMP (2 MBq/head) was intravenously injected to the mice once at Day 0. The body weight and tumor size were measured at least twice a week for a month. Tumor volume (mm^3) was calculated as (length×width^2)/2. In the case of weight loss more than 20%, appearing moribund state signs, or the tumor size greater than 800 mm^3, the mouse was euthanized humanely using isoflurane inhalation. Survival proportion was analyzed by Kaplan-Meier analysis (GraphPad Prism 6, Graph Pad Software, San Diego, CA, USA).

Statistical Analysis

Results are expressed as mean±standard error (SEM). The statistical significance of differences between two groups was calculated using the unpaired Student's t-test. The significance of differences was determined by a one-way analysis of variance (ANOVA), followed by Dunnett's test for multigroup comparisons. The survival curves for [^{211}At]-2-AAMP treatment were compared with that for the control group using the log-rank test. The criterion of significance was $P<0.05$, as determined with GraphPad Prism 6 software.

Results

Radiosynthesis of [^{211}At]-2-AAMP

[^{211}At]-2-AAMP was prepared from the same stannyl precursor and method as used for [^{76}Br]-2-BAMP in 2 step reaction (Fig. 1). Although the first-step reaction proceeded in high radiochemical yield (>95%, Fig. S1), total radiochemical yield of [^{211}At]-2-AAMP determined by TLC was 20.9±3.3%. Since [^{211}At]-2-AAMP isolated by RP-HPLC purification was partially decomposed before being used for further studies, ascorbic acid (final concentration, ≤1%) was added to the solution of [^{211}At]-2-AAMP. As a result, [^{211}At]-2-AAMP was obtained with radiochemical purity greater than 95% (Fig. 2a).

Stability of [^{211}At]-2-AAMP

When [^{211}At]-2-AAMP was incubated in freshly prepared mouse plasma for 6 h at 37°C, 93.7 ±4.4% of radioactivity remained as the intact compound (Fig. 2b). TLC analysis of urine collected up to 1 h after injection of [^{211}At]-2-AAMP showed that more than 90% of the radioactivity remained intact.

Cellular uptake and release of [^{211}At]-2-AAMP

As shown in Fig. 3a, the expression of LAT1 and CD98 was observed in SKOV3 cell. Time-course study showed that [^{211}At]-2-AAMP was rapidly taken up into SKOV3 cells within 10 min, and the uptake was saturated at 20 min after addition (Fig. 3b). There was no difference between HBSS and sodium-free HBSS, indicating that sodium-ion was not involved in cellular uptake of [^{211}At]-2-AAMP (Fig. 3c). Competitive inhibition of [^{211}At]-2-AAMP with various inhibitors showed that the uptake of [^{211}At]-2-AAMP was significantly inhibited by treatment with AMT, a selective inhibitor of LAT1, as well as substrates of LAT1, such as branched-chain amino acids and aromatic amino acids (Fig. 3d). As shown in Fig. 3e, [^{211}At]-2-AAMP was gradually released to extracellular space, and the released fraction reached more than 90% within 60 min after exchanging the buffer.

Cytotoxic effects of [^{211}At]-2-AAMP in tumor cell

[^{211}At]-2-AAMP suppressed clonogenic growth of SKOV3 in a dose-dependent manner. Growth was suppressed from 10 kBq/ml, and was suppressed to only 7.46±2.46% of control at 50 kBq/ml (Fig. 4a). Cell death detected by extracellular release of LDH was observed at 25 kBq/ml of [^{211}At]-2-AAMP, and that became more remarkable at 50 kBq/ml (Fig. 4b). DNA-DSB was also examined after treatment with [^{211}At]-2-AAMP. The comet tail was observed and the intensity of the comet tail was significantly increased after treatment with [^{211}At]-2-AAMP ($P<0.001$, vs control) (Fig. 4c).

Biodistribution study

Table 1 shows biodistribution of [^{211}At]-2-AAMP in SKOV3-bearing mice. Neck was extracted to examine distribution in the thyroid. [^{211}At]-2-AAMP was highly distributed in the kidney and pancreas, and rapidly excreted from the body with lapse of time. Slight retention in the stomach was observed at 6 h. [^{211}At]-2-AAMP also accumulated in the tumor, but the kinetics was different from normal organs. The peak of tumor distribution of [^{211}At]-2-AAMP was 4.34±1.63%ID/g of organ at 30 min and retained high level until 60 min after injection. Then, radioactivity was rapidly eliminated from the tumor.

Table 1 Biodistribution of [^{211}At]-2-AAMP in tumor-bearing mice.

	Time after administration				
	10 min	30 min	60 min	180 min	360 min
Blood	2.63 ± 0.16	1.68 ± 0.13	0.66 ± 0.08	0.07 ± 0.01	0.03 ± 0.00
Liver	3.00 ± 0.21	1.65 ± 0.17	0.65 ± 0.11	0.05 ± 0.01	0.02 ± 0.01
Kidney	8.19 ± 0.53	5.63 ± 0.43	1.95 ± 0.21	0.10 ± 0.03	0.05 ± 0.01
Intestine	3.47 ± 0.58	2.14 ± 0.09	0.77 ± 0.10	0.15 ± 0.02	0.09 ± 0.04
Spleen	3.13 ± 0.40	2.11 ± 0.23	0.58 ± 0.04	0.12 ± 0.03	0.09 ± 0.02
Pancreas	25.66 ± 4.44	9.21 ± 4.59	3.75 ± 0.67	0.06 ± 0.02	0.03 ± 0.02
Stomach	2.99 ± 0.96	1.62 ± 0.27	0.97 ± 0.08	0.60 ± 0.06	0.70 ± 0.24
Heart	2.75 ± 0.20	1.33 ± 0.16	0.62 ± 0.10	0.06 ± 0.02	0.03 ± 0.02
Lung	2.43 ± 0.28	1.72 ± 0.17	0.72 ± 0.06	0.15 ± 0.01	0.12 ± 0.04
Neck	2.24 ± 0.13	1.28 ± 0.21	0.60 ± 0.10	0.11 ± 0.03	0.05 ± 0.03
Muscle	2.11 ± 0.23	1.60 ± 0.20	0.67 ± 0.11	0.02 ± 0.02	0.01 ± 0.01
Bone	1.61 ± 0.39	1.17 ± 0.12	0.34 ± 0.05	0.03 ± 0.02	0.02 ± 0.02
Brain	1.01 ± 0.32	0.52 ± 0.08	0.16 ± 0.03	0.00 ± 0.00	0.00 ± 0.00
Tumor	3.03 ± 0.24	4.34 ± 0.94	2.44 ± 0.42	0.05 ± 0.02	0.02 ± 0.02

Each value represents the mean %injected dose per gram organ±SEM (n=3, 30 min; n=4, other time points).

Therapeutic effects in tumor-bearing mice

In our preliminary examination with small number of mice, weight loss more than 20% was not observed after injection of [^{211}At]-2-AAMP up to 2 MBq (Fig. S2). Therefore, we examined therapeutic response with 2 MBq of [^{211}At]-2-AAMP. Trend to delay of tumor growth was observed after [^{211}At]-2-AAMP treatment and 1 of 5 mice kept tumor growth free survival during the follow-up period. However, there was no significant difference of tumor volume between 2 groups (Fig. 5a and b). Body weight was transiently reduced after treatment with [^{211}At]-2-AAMP (Fig. 5c and d). The peak of weight loss was at 3 days after injection, and the maximum reduction was 14.5%. Kaplan-Meyer survival analysis showed that the survival of mice was significantly improved with [^{211}At]-2-AAMP treatment (Fig. 6, $P<0.05$).

Discussion

In the present study, we newly synthesized [^{211}At]-2-AAMP and evaluated its potential as an α-emitting radiopharmaceutical applicable for treatment of broad range of cancers. Previously, Meyer GJ et al. has successfully developed ^{211}At-labeled amino acid derivative, 4-[^{211}At]astato-L-phenylalanine, and its therapeutic effect in vivo [17, 18]. However, L-phenylalanine is a substrate for not only LAT1, but also LAT2 [19]. In this regard, this is the first report of a LAT1-specific ^{211}At-labeled amino acid derivative. In general, astatinated aryl compounds can be prepared by the procedure similar to be used for radioiodinated and radiobrominated compounds. Thus, [^{211}At]-2-AAMP was prepared according to the procedure similar to that of [^{76}Br]-2-BAMP. The first-step reaction gave the intermediate (Prot-[^{211}At]-2-AAMP) in high yield, whereas the following deprotection reaction reduced the radiochemical yield of [^{211}At]-2-AAMP (20.9 ± 3.3%). This low yield of deprotection reaction was not observed in case of [^{76}Br]-2-

BAMP. Since the complete deprotection of Prot-[^{211}At]-2-AAMP was confirmed by RP-HPLC, the C-At bond would be decomposed during the deprotection reaction. Indeed, [^{211}At]-2-AAMP was sensitive to radiolysis, and partially decomposed after the isolation by RP-HPLC. The addition of ascorbic acid prevented the radiolytic decomposition, and provided [^{211}At]-2-AAMP with radiochemical purity greater than 95%.

Cellular uptake of [^{211}At]-2-AAMP was rapid and sodium-independent, and significantly inhibited with LAT1 selective inhibitors indicating that [^{211}At]-2-AAMP was taken up to cells via LAT1. Since cellular uptake of [^{211}At]-2-AAMP was inhibited in similar pattern with those of [^{76}Br]-2-BAMP and [^{18}F]-2-FAMP [13, 14], differences of halogen would less affect LAT1-selectivity of halogenated α-methyl-L-phenylalanine. Over 90% of [^{211}At]-2-AAMP in cell was released within 60 min in extracellular release study. Since [^{76}Br]-2-BAMP was not involved in the protein synthesis [13], [^{211}At]-2-AAMP would be also hardly used for protein synthesis and this property seem to be a cause of low intracellular retention.

In the biodistribution study, [^{211}At]-2-AAMP showed high accumulation and a certain level of retention in the tumor. Since LAT1 is an amino acid exchanger, tumor accumulation level gradually decreased with blood clearance [20]. However, rapid blood clearance of [^{211}At]-2-AAMP achieved high tumor-to-blood ratio (3.65 ± 0.18 at 1 h after injection) and rapid clearance from the body which is favorable property for radionuclide therapy. [^{211}At]-2-AAMP was highly distributed in the kidney and pancreas soon after injection, then it was rapidly eliminated from these organs. These biodistribution patterns were similar with [^{76}Br]-2-BAMP and [^{18}F]-2-FAMP. In the study of RNA sequencing in human normal tissues (https://www.ncbi.nlm.nih.gov/gene/8140), the expression of LAT1 mRNA is also relatively low in pancreas compared to the other organs [21]. No significant uptake of [^{123}I]-3-iodo or [^{18}F]-3-fluoro-α-methyltyrosine, other LAT1 specific tracers, was not observed in the human pancreas [22, 23]. Therefore, the high distribution in the pancreas will not be expected in patients. Dehalogenation of [^{211}At]-labeled radiopharmaceuticals to release free ^{211}At is one of main problems for clinical use since free ^{211}At generally accumulate and remain in the spleen, thyroid, lung and stomach which causes side effect [24–26]. In this study, small amounts of radioactivity were retained in the stomach and [^{211}At]-2-AAMP was remained as intact in murine plasma for 6 h. Greater than 90% of radioactivity was excreted into the urine as intact. These results suggest that [^{211}At]-2-AAMP remained stable in vivo. Although future studies of [^{211}At]-2-AAMP in patients are necessary, these results suggested low radiation exposure to other organs to cause little side effect.

In vitro assessments of therapeutic effect, [^{211}At]-2-AAMP suppressed clonogenic growth and also induced cell death. DNA-DSB after treatment with [^{211}At]-2-AAMP indicates that cytotoxicity of [^{211}At]-2-AAMP was caused by α-radiation. In addition, [^{211}At]-2-AAMP significantly improved survival rates of mice in vivo. These results suggest that [^{211}At]-2-AAMP is possibly beneficial for treatment of LAT1-positive cancer. However, significant delay or reduction of tumor size was not observed by treatment with [^{211}At]-2-AAMP in vivo partially because small number of mice. Since the body weight loss after 2 MBq of

[^{211}At]-2-AAMP injection was not large and the present administration dose did not reach the maximum tolerated dose, suggesting that higher doses would be safely administered to improve the therapeutic effect with. Thus, the administration of higher dose would be possible and which would improve therapeutic effect. However, studies with more than 2 MBq/head of [^{211}At]-2-AAMP was not performed because of limited available radioactivity of ^{211}At and the low radiolabeling yield of [^{211}At]-2-AAMP. Further improvements in radiolabeling method will be needed to estimate the therapeutic effect of [^{211}At]-2-AAMP at higher doses. Another concern is that the clearance of [^{211}At]-2-AAMP from tumor might be too rapid to give enough radiation for suppressing tumor growth. Therefore, modification of [^{211}At]-2-AAMP itself or combination with other compound to improve tumor retention of [^{211}At]-2-AAMP would constitute a strategy for better therapeutic effect. It was reported that pre-injection of probenecid, an organic anion transporter inhibitor enhances tumor accumulation levels of amino acid tracer in tumor-bearing mice [27] or pre-loading of a certain kind of amino acid enhance the tumor cell uptake of amino acid tracer [28]. Such kinds of approach could be applied to [^{211}At]-2-AAMP, and would enhance tumor accumulation level which enable to improve therapeutic effect.

Conclusion

We prepared [^{211}At]-2-AAMP from the stannyl precursor, and showed α-radiation-dependent cellular growth inhibition after taking up via LAT1. In addition, [^{211}At]-2-AAMP significantly improved the survival of tumor-bearing mice. These results suggest that [^{211}At]-2-AAMP would be useful for treatment of LAT1-positive cancers.

Declarations

Ethical Approval and Consent to participate

All applicable international, national, and/or institutional guidelines for the care and use of animals were followed. Animal experimental protocol was approved by the Institutional Animal Care and Use Committee at our facility (19-T001-1). This article does not contain any studies with human participants performed by any of the authors.

Consent for publication

Not applicable

Availability of supporting data

All data generated or analyzed during this study are included in this published article [and its supplementary information files].

Competing interests

The authors declare that they have no conflict of interest.

Funding

This work was supported by JSPS KAKENHI grant 18H02760 to Hirofumi Hanaoka.

Authors' contributions

All authors contributed to the study conception and design. Material preparation, data collection and analysis were performed by Yasuhiro Ohshima, Hiroyuki Suzuki, Hirofumi Hanaoka, Ichiro Sasaki, Shigeki Watanabe, Hiromitsu Haba, and Noriko S. Ishioka. The first draft of the manuscript was written by Yasuhiro Ohshima and all authors commented on previous versions of the manuscript. All authors read and approved the final manuscript.

Acknowledgements

The authors thank the staff in the cyclotron operation section for the cyclotron operation.

References

1. McDevitt MR, Sgouros G, Sofou S. Targeted and Nontargeted α-Particle Therapies. Annu Rev Biomed Eng. 2018;20:73-93.
2. Makvandi M, Dupis E, Engle JW, Nortier FM, Fassbender ME, Simon S, et al. Alpha-Emitters and Targeted Alpha Therapy in Oncology: from Basic Science to Clinical Investigations. Target Oncol. 2018;13:189-203.
3. Lorat Y, Brunner CU, Schanz S, Jakob B, Taucher-Scholz G, Rübe CE. Nanoscale analysis of clustered DNA damage after high-LET irradiation by quantitative electron microscopy–the heavy burden to repair. DNA Repair. 2015;28:93-106.
4. Marcu L, Bezak E, Allen BJ. Global comparison of targeted alpha vs targeted beta therapy for cancer: In vitro, in vivo and clinical trials. Crit Rev Oncol Hematol. 2018;123:7-20.

5. Rosenblat TL, McDevitt MR, Mulford DA, Pandit-Taskar N, Divgi CR, Panageas KS, et al. Sequential cytarabine and alpha-particle immunotherapy with bismuth-213-lintuzumab (HuM195) for acute myeloid leukemia. Clin Cancer Res. 2010;16:5303-11.
6. Kratochwil C, Bruchertseifer F, Giesel FL, Weis M, Verburg FA, Mottaghy F, et al. 225Ac-PSMA-617 for PSMA-Targeted α-Radiation Therapy of Metastatic Castration-Resistant Prostate Cancer. J Nucl Med. 2016;57:1941-4.
7. Kratochwil C, Giesel FL, Bruchertseifer F, Mier W, Apostolidis C, Boll R, et al. ^{213}Bi-DOTATOC receptor-targeted alpha-radionuclide therapy induces remission in neuroendocrine tumours refractory to beta radiation: a first-in-human experience. Eur J Nucl Med Mol Imaging. 2014;41:2106-19.
8. Wullschleger S, Loewith R, Hall MN. TOR signaling in growth and metabolism. 2006;124:471-84.
9. Yanagida O, Kanai Y, Chairoungdua A, Kim DK, Segawa H, Nii T, et al. Human L-type amino acid transporter 1 (LAT1): characterization of function and expression in tumor cell lines. Biochim Biophys Acta. 2001;1514:291-302.
10. Häfliger P, Charles RP, The L-Type Amino Acid Transporter LAT1-An Emerging Target in Cancer. Int J Mol Sci. 2019;20:E2428.
11. Ohshima Y, Hanaoka H, Watanabe S, Sugo Y, Watanabe S, Tominaga H, et al. Preparation and biological evaluation of 3-[(76)Br]bromo-α-methyl-L-tyrosine, a novel tyrosine analog for positron emission tomography imaging of tumors. Nucl Med Biol. 2011;38:857-65.
12. Ohshima Y, Hanaoka H, Tominaga H, Kanai Y, Kaira K, Yamaguchi A, et al. Biological evaluation of 3-[(18)F]fluoro-α-methyl-D-tyrosine (D-[(18)F]FAMT) as a novel amino acid tracer for positron emission tomography. Ann Nucl Med. 2013;27:314-24.
13. Hanaoka H, Ohshima Y, Suzuki Y, Yamaguchi A, Watanabe S, Uehara T, et al. Development of a Widely Usable Amino Acid Tracer: ⍰⍰Br-α-Methyl-Phenylalanine for Tumor PET Imaging. J Nucl Med. 2015;56:791-7.
14. Hanaoka H, Ohshima Y, Yamaguchi A, Suzuki H, Ishioka NS, Higuchi T, et al. Novel 18F-Labeled α-Methyl-Phenylalanine Derivative with High Tumor Accumulation and Ideal Pharmacokinetics for Tumor-Specific Imaging. Mol Pharm. 2019;16:3609-16.
15. Vaidyanathan G, Zalutsky MR. 1-(m-[211At]astatobenzyl)guanidine: synthesis via astato demetalation and preliminary in vitro and in vivo evaluation. Bioconjug Chem. 1992;3:499-503.
16. Morimoto E, Kanai Y, Kim DK, Chairoungdua A, Choi HW, Wempe MF, et al. Establishment and characterization of mammalian cell lines stably expressing human L-type amino acid transporters. J Pharmacol Sci. 2008;108:505-16.
17. Meyer GJ, Walte A, Sriyapureddy SR, Grote M, Krull D, Korkmaz Z, et al. Synthesis and analysis of 2-[211At]-L-phenylalanine and 4-[211At]-L-phenylalanine and their uptake in human glioma cell cultures in-vitro. Appl Radiat Isot. 2010;68:1060-5.
18. Borrmann N, Friedrich S, Schwabe K, Hedrich HJ, Krauss JK, Knapp WH, et al. Systemic treatment with 4-211Atphenylalanine enhances survival of rats with intracranial glioblastoma. Nuklearmedizin. 2013;52:212-21.

19. Segawa H, Fukasawa Y, Miyamoto K, Takeda E, Endou H, Kanai Y. Identification and functional characterization of a Na+-independent neutral amino acid transporter with broad substrate selectivity. J Biol Chem. 1999;274:19745-51.
20. Meier C, Ristic Z, Klauser S, Verrey F. Activation of system L heterodimeric amino acid exchangers by intracellular substrates. EMBO J. 2002;21:580-9.
21. Fagerberg L, Hallström BM, Oksvold P, Kampf C, Djureinovic D, Odeberg J, et al. Analysis of the human tissue-specific expression by genome-wide integration of transcriptomics and antibody-based proteomics. Mol Cell Proteomics. 2014;13:397-406.
22. Langen KJ, Pauleit D, Coenen HH. 3-[123I]iodo-alpha-methyl-L-tyrosine: uptake mechanisms and clinical applications. Nucl Med Biol. 2002;29:625-31.
23. Inoue T. Koyama K. Oriuchi N. Alyafei S. Yuan Z. Suzuki H, et al. Detection of malignant tumors: whole-body PET with fluorine 18 alpha-methyl tyrosine versus FDG–preliminary study. Radiology. 2001;220:54–62.
24. Garg PK, Harrison CL, Zalutsky MR. Comparative tissue distribution in mice of the alpha-emitter 211At and 131I as labels of a monoclonal antibody and F(ab')2 fragment. Cancer Res. 1990;50:3514-20.
25. Larsen RH, Murud KM, Akabani G, Hoff P, Bruland OS, Zalutsky MR. 211At- and 131I-labeled bisphosphonates with high in vivo stability and bone accumulation. J Nucl Med. 1999;40:1197-203.
26. Spetz J, Rudqvist N, Forssell-Aronsson E, Biodistribution and dosimetry of free 211At, 125I- and 131I- in rats. Cancer Biother Radiopharm. 2013;28:657-64.
27. Nakajima S, Shikano N, Kotani T, Ogura M, Nishii R, Yoshimoto M, et al. Pharmacokinetics of 3-[125I]iodo-alpha-methyl-L-tyrosine, a tumor imaging agent, after probenecid loading in mice implanted with colon cancer DLD-1 cells. Nucl Med Biol. 2007;34:1003-8.
28. Wingelhofer B, Kreis K, Mairinger S, Muchitsch V, Stanek J, Wanek T, et al. Preloading with L-BPA, L-tyrosine and L-DOPA enhances the uptake of [18F]FBPA in human and mouse tumour cell lines. Appl Radiat Isot. 2016;118:67-72.

Figures

Fig. 1

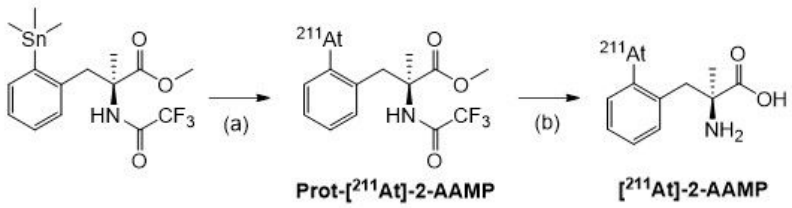

Figure 1

Synthetic scheme of [211At]-2-AAMP. Reagents and conditions: (a) 1) aqueous solution of 211At, NCS, methanol, rt for 15 min; 2) aqueous solution of sodium bisulfite; (b) 6N NaOH 70°C for 1 h

Fig. 2

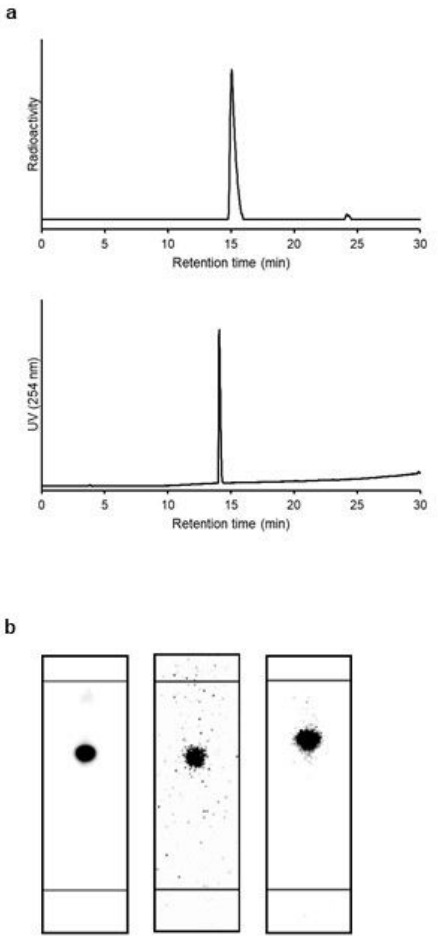

Figure 2

RP-HPLC and TLC analyses of [211At]-2-AAMP. (a) RP-HPLC profiles of [211At]-2-AAMP (top) and 2-IAMP (bottom). (b) TLC radiochromatograms of standard sample of [211At]-2-AAMP (left), [211At]-2-AAMP after incubation in murine plasma for 6 h (center) and the urine sample collected for 1 h after injection of [211At]-2-AAMP (right)

Fig. 3

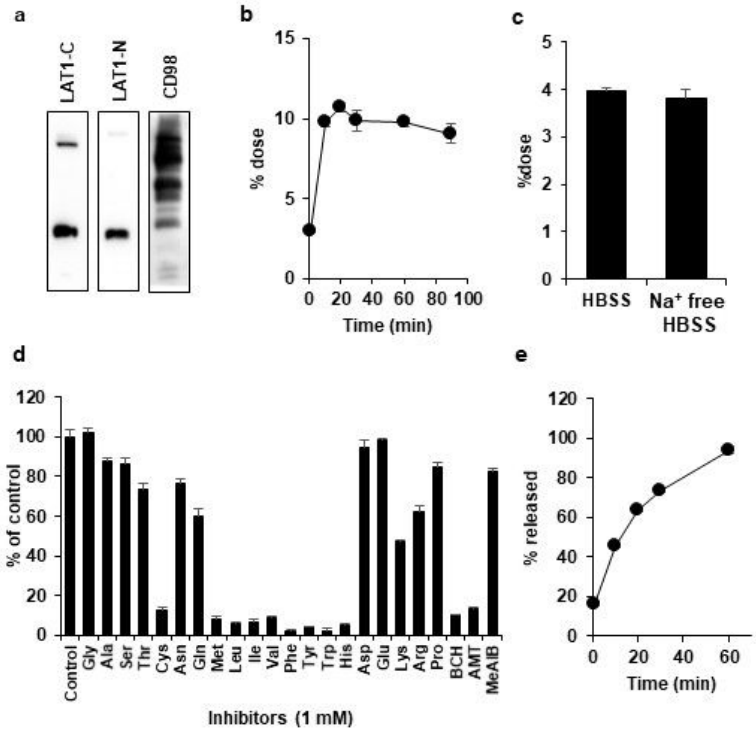

Figure 3

Cellular uptake and release of [211At]-2-AAMP in SKOV3 expressing LAT1. (a) Expression of LAT1 and CD98 in SKOV3 cells. LAT1-C shows bands detected with rabbit anti-LAT1 carboxyl-terminal antibody, and LAT1-N shows bands detected with rabbit anti-LAT1 amino-terminal antibody. (b) Time-course study of [211At]-2-AAMP uptake (n=4). (c) [211At]-2-AAMP uptake in presence or absence of sodium-ion (n=4). Y-axis shows a percent of applied dose of [211At]-2-AAMP. (d) Inhibition of [211At]-2-AAMP uptake with

amino acids and LAT1 selective inhibitor (n=4). Y-axis shows present of control. The inhibitors are as follow. Ala = alanine; AMT = α-methyl-L-tyrosine; Arg = arginine; Asn = asparagine; Asp = aspartic acid; BCH = 2-aminobicyclo-(2,2,1)-heptane-2-carboxylic acid; Cont = control; Cys = cysteine; Gln = glutamine; Glu = glutamic acid; Gly = glycine; His = histidine; Ile = isoleucine; Leu = leucine; Lys = lysine; MeAIB = α-methyl-aminoisobutyric acid; Met = methionine; Phe = phenylalanine; Pro = proline; Ser = serine; Thr = threonine; Trp = tryptophan; Tyr = tyrosine; Val = valine. (e) Extracellular release of [211At]-2-AAMP (n=4). Y-axis shows a percent of release of [211At]-2-AAMP

Fig. 4

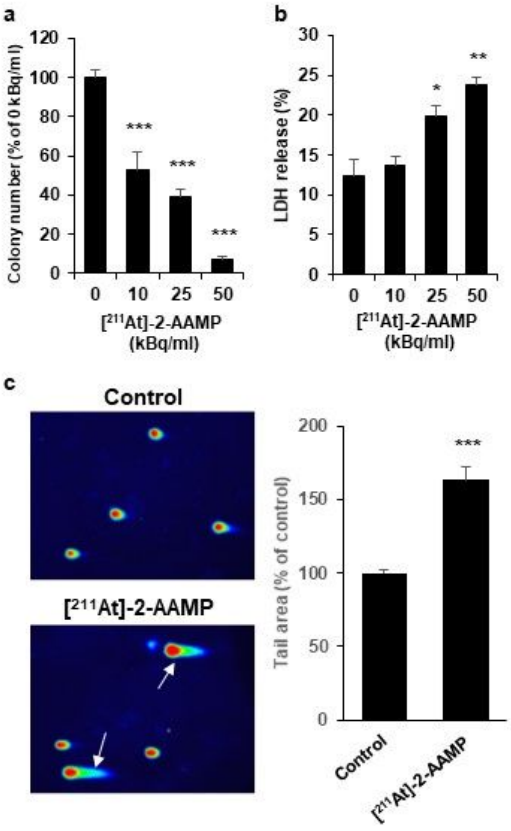

Figure 4

In vitro cytotoxicity of [211At]-2-AAMP. Clonogenic growth of SKOV3 (a) and extracellular release of LDH (b) after treatment with 0, 10, 25, 50 kBq/ml of [211At]-2-AAMP (n=4). Colony number was shown as percent of untreated control (0 kBq/ml). (c) Cells with DNA-DSB after treatment with 25 kBq/ml of [211At]-2-AAMP. The arrows indicate the representative comets with DNA-DSB. DNA-DSB was quantified by determining tail area of the comet. A statistically significant difference from the control is indicated by * ($P < 0.01$), ** ($P < 0.005$), or *** ($P < 0.001$)

Fig. 5

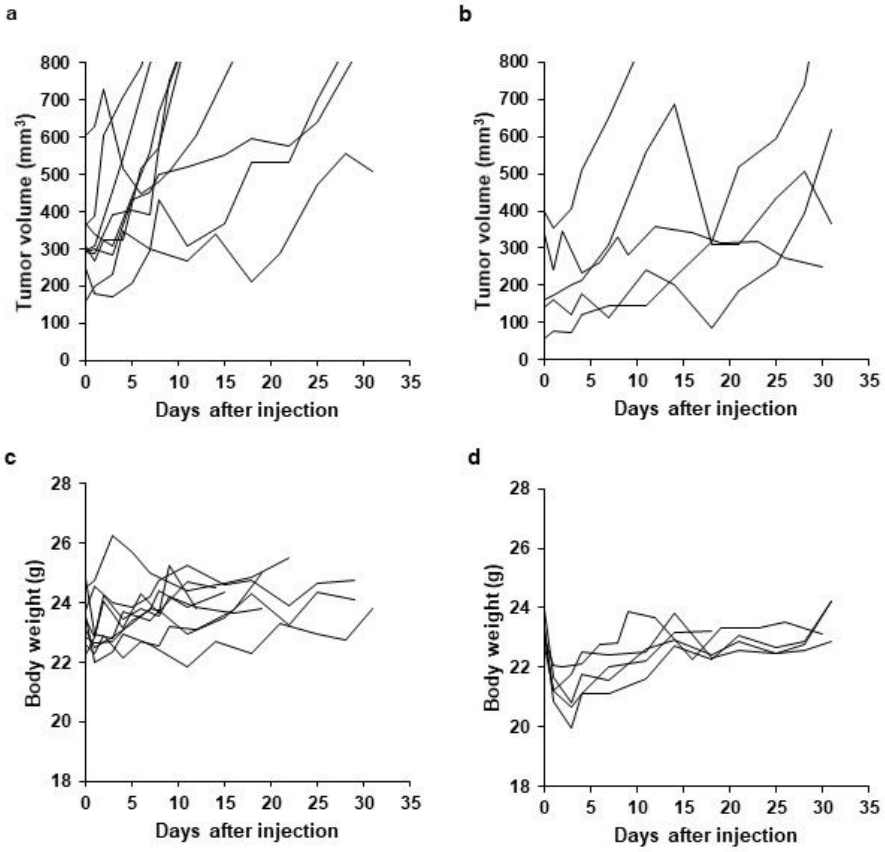

Figure 5

Effects of [211At]-2-AAMP on tumor volume and body weight. Tumor growth and body weight of each mouse after treatment with 2 MBq of [211At]-2-AAMP (b and d, n=5) or untreatment (a and c, n=9)

Fig. 6

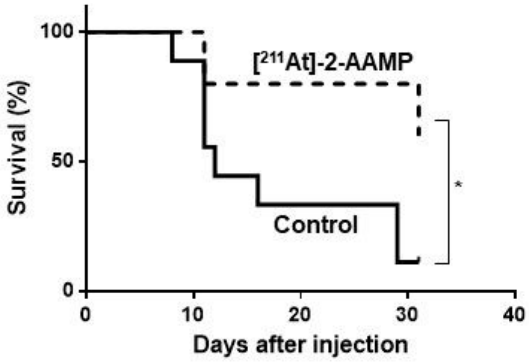

Figure 6

Kaplan-Meier survival curves. The group treated with 2 MBq of [211At]-2-AAMP showed significantly better survival than the control group (* P < 0.05 vs. control)

Supplementary Files

This is a list of supplementary files associated with this preprint. Click to download.

- SupplementarymaterialsEJNMMIYO.docx